

## Single-dose replicating RNA vaccine induces neutralizing antibodies against SARS-CoV-2 in nonhuman primates

Jesse H. Erasmus<sup>1,2</sup>, Amit P. Khandhar<sup>2,3</sup>, Alexandra C. Walls<sup>6</sup>, Emily A. Hemann<sup>5,8</sup>, Megan A. O'Connor<sup>1,7</sup>, Patience Murapa<sup>1</sup>, Jacob Archer<sup>1,3</sup>, Shanna Leventhal<sup>4</sup>, Jim Fuller<sup>1</sup>, Thomas Lewis<sup>1,7</sup>, Kevin E. Draves<sup>1</sup>, Samantha Randall<sup>3</sup>, Kathryn A. Guerriero<sup>7</sup>, Malcolm S. Duthie<sup>2</sup>, Darrick Carter<sup>2,3,5</sup>, Steven G. Reed<sup>3,5</sup> David W. Hawman<sup>4</sup>, Heinz Feldmann<sup>4</sup>, Michael Gale, Jr.<sup>5,7,8</sup>, David Veessler<sup>6</sup>, Peter Berglund<sup>2</sup>, Deborah Heydenburg Fuller<sup>1,5,7\*</sup>.

<sup>1</sup>Department of Microbiology, University of Washington, Seattle, WA

<sup>2</sup>Host Directed Therapeutics (HDT) Bio Corp, Seattle, WA

<sup>3</sup>PAI Life Sciences, Seattle, WA

<sup>4</sup>Laboratory of Virology, Division of Intramural Research, National Institute of Allergy and Infectious Diseases, National Institutes of Health, Hamilton, MT

<sup>5</sup>Center for Innate Immunity and Immune Disease, University of Washington, Seattle, WA

<sup>6</sup>Department of Biochemistry, University of Washington, Seattle, WA

<sup>7</sup>Washington National Primate Research Center, Seattle, WA

<sup>8</sup>Department of Immunology, University of Washington, Seattle, WA

\*Corresponding author:

Deborah Heydenburg Fuller

Professor, Department of Microbiology, University of Washington, Seattle, WA

Division Chief, Infectious Diseases and Translational Medicine, Washington National Research Primate Research Center, Seattle, WA

[fullerdh@uw.edu](mailto:fullerdh@uw.edu)

Running title: Replicating RNA Vaccine for COVID-19

Keywords for submission: coronavirus; SARS-CoV-2; vaccine; RNA; replicon; nanoparticle; nonhuman primates.

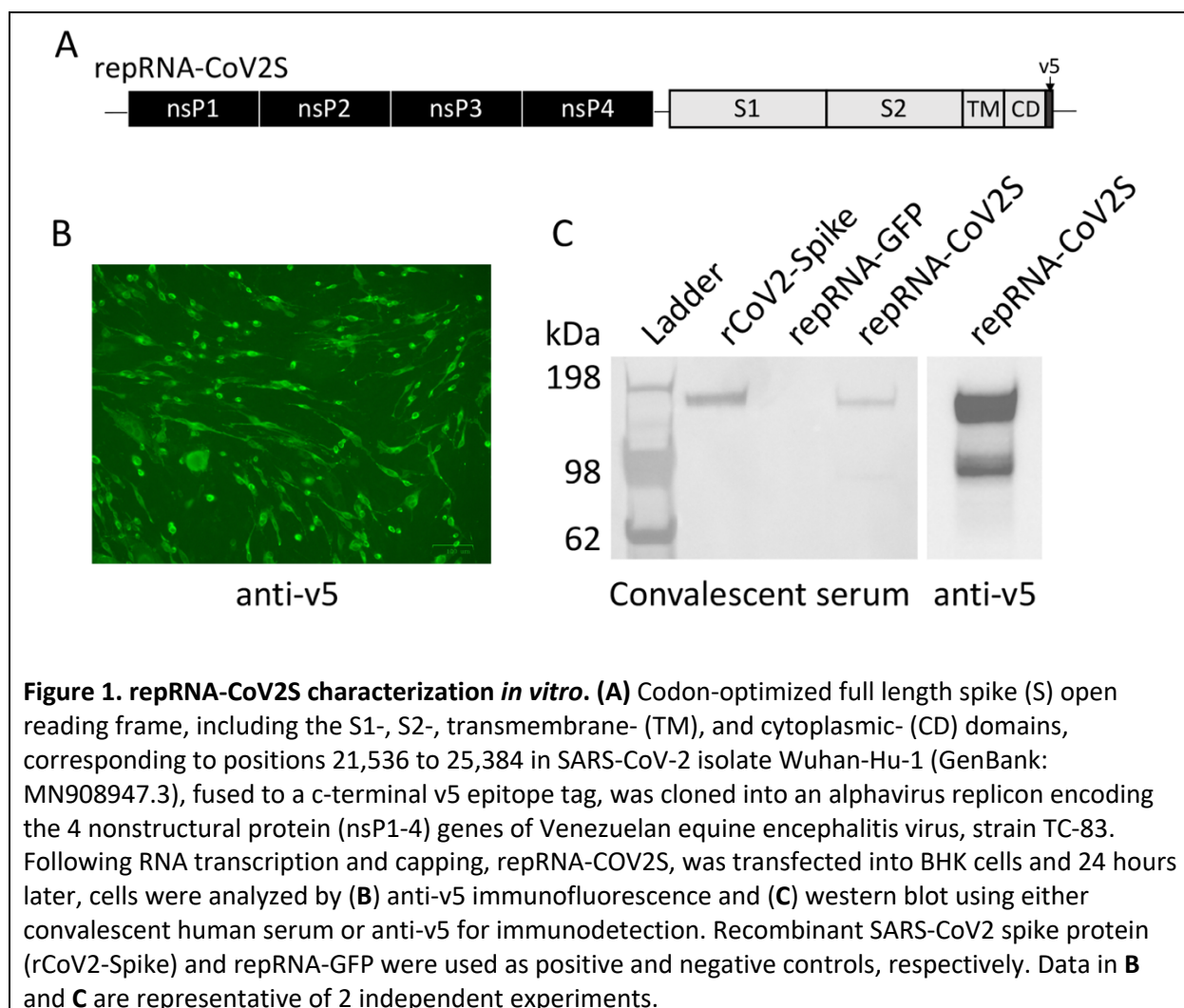
1 **Abstract**

2           The ongoing COVID-19 pandemic, caused by infection with SARS-CoV-2, is having a dramatic and  
3 deleterious impact on health services and the global economy. Grim public health statistics highlight the  
4 need for vaccines that can rapidly confer protection after a single dose and be manufactured using  
5 components suitable for scale-up and efficient distribution. In response, we have rapidly developed  
6 repRNA-CoV2S, a stable and highly immunogenic vaccine candidate comprised of an RNA replicon  
7 formulated with a novel Lipid InOrganic Nanoparticle (LION) designed to enhance vaccine stability,  
8 delivery and immunogenicity. We show that intramuscular injection of LION/repRNA-CoV2S elicits  
9 robust anti-SARS-CoV-2 spike protein IgG antibody isotypes indicative of a Type 1 T helper response as  
10 well as potent T cell responses in mice. Importantly, a single-dose administration in nonhuman primates  
11 elicited antibody responses that potently neutralized SARS-CoV-2. These data support further  
12 development of LION/repRNA-CoV2S as a vaccine candidate for prophylactic protection from SARS-CoV-  
13 2 infection.

14 Severe acute respiratory syndrome coronavirus-2 (SARS-CoV-2) first emerged in December 2019  
15 and within 3 months, Coronavirus Disease 2019 (COVID-19), caused by SARS-CoV-2 infection, was  
16 declared a worldwide pandemic<sup>1-3</sup>. Coronaviruses are enveloped, single-strand positive-sense RNA  
17 viruses with a large genome and open reading frames for four major structural proteins: Spike (S),  
18 envelope, membrane, and nucleocapsid. The S protein mediates binding of coronaviruses to angiotensin  
19 converting enzyme 2 (ACE2) on the surface of various cell types including epithelial cells of  
20 the pulmonary alveolus<sup>4-6</sup>. Protection is thought to be mediated by neutralizing antibodies against the S  
21 protein<sup>7,8</sup>, as most of the experimental vaccines developed against the related SARS-CoV incorporated  
22 the S protein, or its receptor binding domain (RBD), with the goal of inducing robust, neutralizing  
23 responses<sup>9-11</sup>. Indeed, previous reports have shown that human neutralizing antibodies protected mice  
24 challenged with SARS-CoV<sup>12-14</sup> and Middle East respiratory syndrome (MERS)-CoV<sup>15</sup> suggesting that  
25 protection against SARS-CoV-2 can be mediated through anti-S antibodies. Additionally, SARS vaccines  
26 that drive Type 2 T helper (Th2) responses have been associated with enhanced lung immunopathology  
27 following challenge with SARS-CoV while those with a Type 1 T helper (Th1)-biased immune response  
28 are associated with enhanced protection in the absence of immunopathology<sup>16,17</sup>. Therefore, an  
29 effective COVID-19 vaccine will likely need to induce, at the very least, Th1-biased immune responses  
30 comprised of SARS-CoV-2-specific neutralizing antibodies.

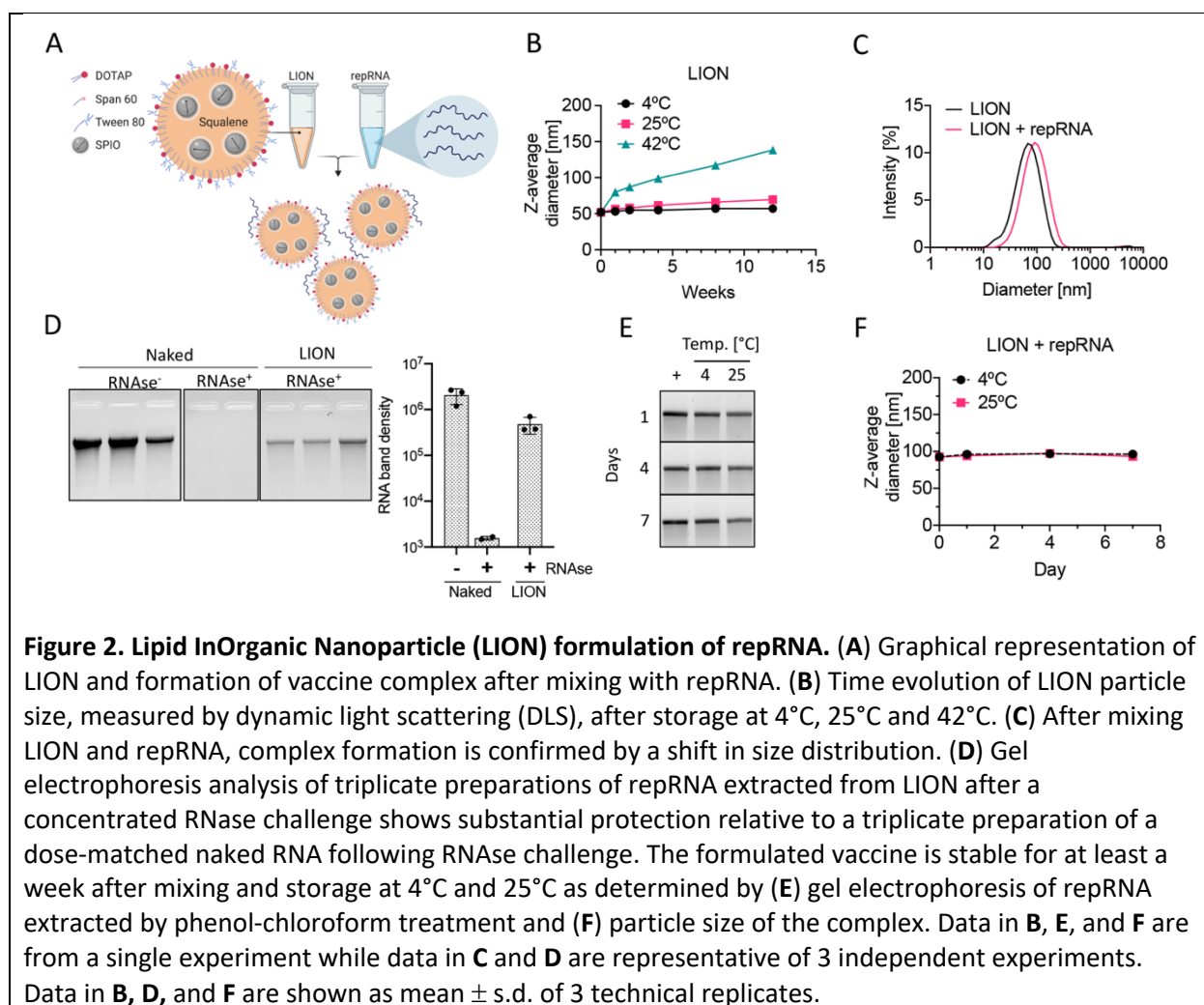
31 Nucleic acid vaccines have emerged as ideal modalities for rapid vaccine design, requiring only  
32 the target antigen's gene sequence and removing dependence on pathogen culture (inactivated or live  
33 attenuated vaccines) or scaled recombinant protein production. In addition, nucleic acid vaccines avoid  
34 pre-existing immunity that can dampen immunogenicity of viral vectored vaccines. Recently, clinical  
35 trials were initiated with messenger RNA (mRNA) vaccines formulated with lipid nanoparticles (LNPs)  
36 and a DNA vaccine delivered by electroporation<sup>18</sup>. However, mRNA and DNA vaccines may not be able  
37 to induce protective efficacy in humans after a single immunization since, similar to inactivated and  
38 recombinant subunit protein vaccines, they typically require multiple administrations over an extended  
39 period of time to become effective<sup>19</sup>. Virus-derived replicon RNA (repRNA) vaccines were first described  
40 in 1989 and have been delivered in the forms of virus-like RNA particles (VRP), *in-vitro* transcribed (IVT)  
41 RNA, and plasmid DNA<sup>20-23</sup>. In repRNA the open reading frame encoding the viral RNA polymerase  
42 complex (most commonly from the *Alphavirus* genus) is intact but the structural protein genes are  
43 replaced with an antigen-encoding gene<sup>20,24-26</sup>. While conventional mRNA vaccines, like that initiated in  
44 a recent clinical trial, are translated directly from the incoming RNA molecules, introduction of repRNA  
45 into cells initiates ongoing biosynthesis of antigen-encoding RNA that results in dramatically increased

46 expression and duration that significantly enhances humoral and cellular immune responses<sup>27</sup>. In  
47 addition, repRNA vaccines mimic an alphavirus infection in that viral-sensing stress factors are triggered  
48 and innate pathways are activated through Toll-like receptors and retinoic acid inducible gene (RIG)-I to  
49 produce interferons, pro-inflammatory factors and chemotaxis of antigen-presenting cells, as well as  
50 promoting antigen cross-priming<sup>28</sup>. As a result, repRNA acts as its own adjuvant, eliciting more robust  
51 immune responses after a single dose, relative to conventional mRNA which typically requires multiple  
52 and 1,000-fold higher doses<sup>29</sup>. An effective vaccine to stop a pandemic outbreak like COVID-19 would  
53 ideally induce protective levels of immunity rapidly and after only a single dose while simultaneously  
54 reducing the load on manufacturing at scale, due to a requirement for fewer and lower doses. Since  
55 repRNA vaccines often require only a single administration to be effective<sup>30</sup>, they offer considerable  
56 potential to meet this need.



57

58 Building on experience with the attenuated Venezuelan equine encephalitis virus (VEEV) TC-83  
 59 strain<sup>22,30-34</sup>, we generated repRNAs incorporating sequences from the SARS-CoV-2 Spike (S) protein,  
 60 including full length S (repRNA-CoV2S) (Fig. 1A). Using immunofluorescence and western blot we  
 61 demonstrated efficient expression of the v5-tagged S protein in BHK cells (Fig. 1B,C). Then, utilizing  
 62 convalescent serum collected 29 days after onset of COVID-19 as an immunodetection reagent, we  
 63 demonstrated endogenous expression of an S protein in BHK cells, reactive with natural SARS-CoV-2  
 64 immune sera (Fig. 1C). Next, we evaluated the ability of repRNA-CoV2S to rapidly generate antibody and  
 65 T cell responses in mice when formulated with a novel Lipid InOrganic Nanoparticle (LION) designed to  
 66 enhance vaccine stability and intracellular delivery of the vaccine.

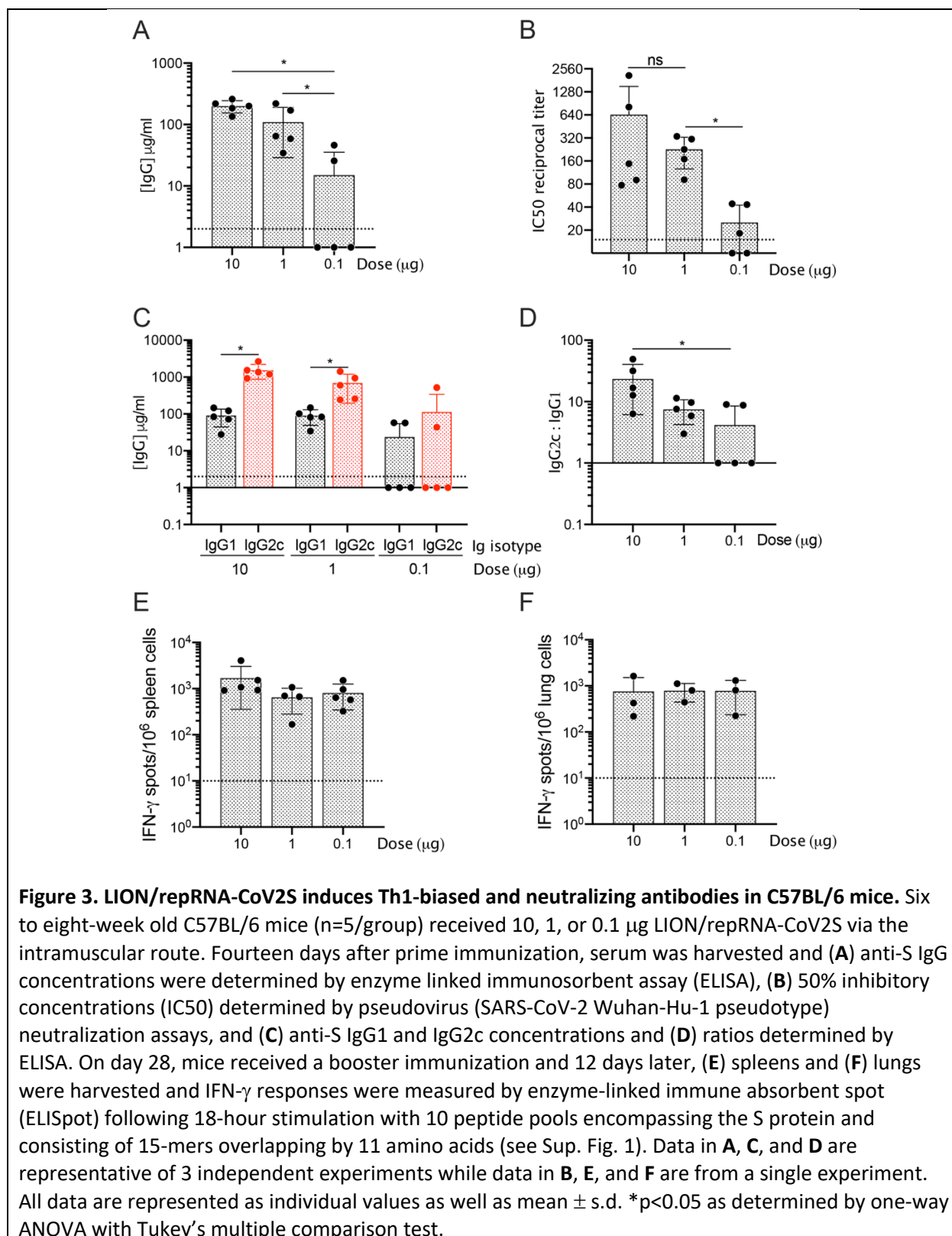


67  
 68 LION is a highly stable cationic squalene emulsion with 15 nm superparamagnetic iron oxide  
 69 (Fe<sub>3</sub>O<sub>4</sub>) nanoparticles (SPIO) embedded in the hydrophobic oil phase. Squalene is a known vaccine  
 70 adjuvant<sup>35,36</sup> and SPIO nanoparticles have a long history of clinical use in MRI contrast and intravenous

71 iron replacement therapy; the unique nonlinear magnetic properties of SPIOs have also been leveraged  
72 for novel use in a range of imaging, targeting and therapy applications<sup>37–42</sup>. A key component of LION is  
73 the cationic lipid 1,2-dioleoyl-3-trimethylammonium propane (DOTAP), which enables electrostatic  
74 association with RNA molecules when combined by a simple 1:1 (v/v) mixing step (Fig. 2A). LION has an  
75 intensity-weighted average diameter of 52 nm (PDI = 0.2) measured by dynamic light scattering (DLS).  
76 The formulation is colloidally stable for at least 3 months when stored at 4 and 25°C (Fig. 2B). When  
77 mixed, electrostatic association between anionic repRNA and cationic DOTAP molecules on the surface  
78 of LION promotes immediate complex formation, as confirmed by increase in particle size to an  
79 intensity-weighted average diameter of 90 nm detected by DLS (Fig. 2C). Gel electrophoresis analysis of  
80 LION-formulated repRNA molecules extracted by phenol-chloroform treatment after a concentrated  
81 RNase challenge showed substantial protection from RNase-catalyzed degradation compared to  
82 unformulated repRNA (Fig. 2D). To evaluate short-term stability of the vaccine, we evaluated repRNA  
83 integrity and complex stability on 1, 4 and 7 days after mixing. LION maintained full integrity of the  
84 repRNA molecules (Fig. 2E) and complex size (Fig. 2F) at all time points.

85         A single intramuscular immunization of C57BL/6 mice with 10 or 1 µg of LION/repRNA-CoV2S  
86 induced 100% seroconversion by 14 days post-immunization and robust anti-S IgG levels with mean  
87 binding titers of 200 and 109 µg/ml, respectively, and partial seroconversion (2 out of 5) at a 0.1 µg dose  
88 (Fig. 3A). Both the 10 and 1 µg prime-only doses induced neutralizing antibodies with mean 50%  
89 inhibitory concentrations (IC50) of 1:643 and 1:226, respectively, as measured by pseudovirus  
90 neutralization assay (SARS-CoV-2 Wuhan-Hu-1 pseudotype). While all doses induced Th1-biased immune  
91 responses indicated by significantly higher IgG2c responses when compared to IgG1 (Fig. 3C), there was  
92 a trend toward higher doses inducing even more Th1-biased responses as indicated by higher IgG2c:IgG1  
93 ratios (Fig. 3D). Given the potential role for T cells to contribute to protection, as seen with SARS and  
94 MERS<sup>43–45</sup>, especially in the presence of waning antibody and memory B cell responses, we also  
95 evaluated T cell responses to LION/repRNA-CoV2S in mice. On day 28 this same cohort of mice received  
96 a second immunization and 12 days later, spleens and lungs were harvested and stimulated with an  
97 overlapping 15-mer peptide library of the S protein, and IFN-γ responses were measured by enzyme-  
98 linked immune absorbent spot (ELISpot) assay. Mice receiving a 10, 1, and 0.1 µg prime/boost exhibited  
99 robust splenic T cell responses with mean IFN-γ spots/10<sup>6</sup> cells of 1698, 650, and 801, respectively (Fig.  
100 3E). Robust T cell responses were also detected in the lung and were similar between groups with mean  
101 IFN-γ spots/10<sup>6</sup> cells of 756, 784, and 777, respectively (Fig. 3F). Interestingly, analysis of the specificity  
102 of peptide response showed a biased response towards the S1 domain of the S protein in the spleen

103 (Sup. Fig. 1A) whereas responses in the lung were more broadly distributed between the S1 and S2  
 104 domains of the S protein (Sup. Fig. 1B).





105 The elderly are among the most vulnerable to COVID-19 but immune senescence in this  
106 population poses a barrier to effective vaccination. To evaluate the effect of immune senescence on  
107 immunogenicity, we next administered 10 or 1  $\mu$ g of LION/repRNA-CoV2S in 2-, 8-, and 17-month old  
108 BALB/C mice and measured anti-S IgG concentrations at 14 days after a single immunization.  
109 Significantly lower antibody titers were observed in the 17-month old mice at both doses (Fig. 4A), when  
110 compared to 2- and 8-month old mice, suggesting that higher doses and/or additional booster doses  
111 may be required in the most immune senescent populations to induce sufficient immunity. No  
112 differences were observed between the 2- and 8-month old mice. Interestingly, although BALB/C mice  
113 tend to develop a more Th2 immune-biased response following vaccination<sup>46</sup>, LION/repRNA-CoV2S  
114 induced ratios of IgG2a:IgG1 greater than 1 (Fig. 4B, C) in all age groups of BALB/C mice, indicating a  
115 Th1-biased immune response. Given that severe, life-threatening COVID-19 appears to be more  
116 common among elderly individuals, irrespective of type of T helper response, and that severe SARS is  
117 associated with skewing toward Th2 antibody profiles with an inadequate Th1 response<sup>16,17,43</sup>, the  
118 ability of LION/repRNA-CoV2S to induce strong and Th1-biased responses in 8- and 2-month old mice,  
119 even in the Th2-biased BALB/c strain, is a promising finding regarding the potential safety and  
120 immunogenicity of this vaccine.

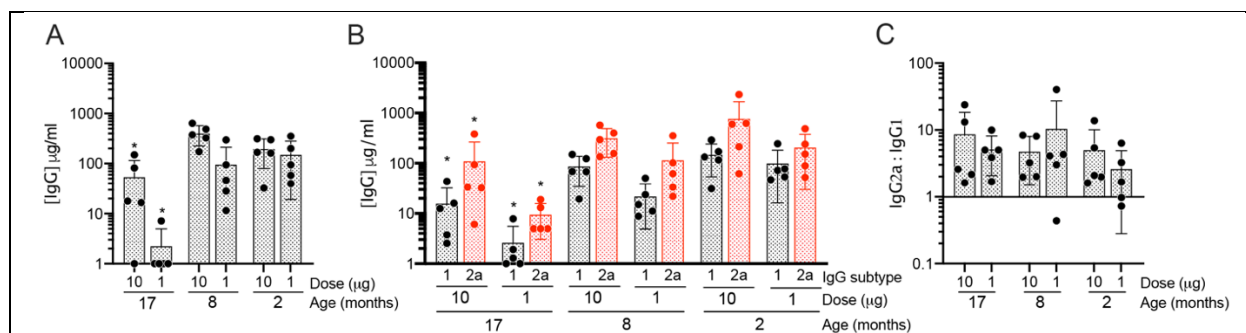
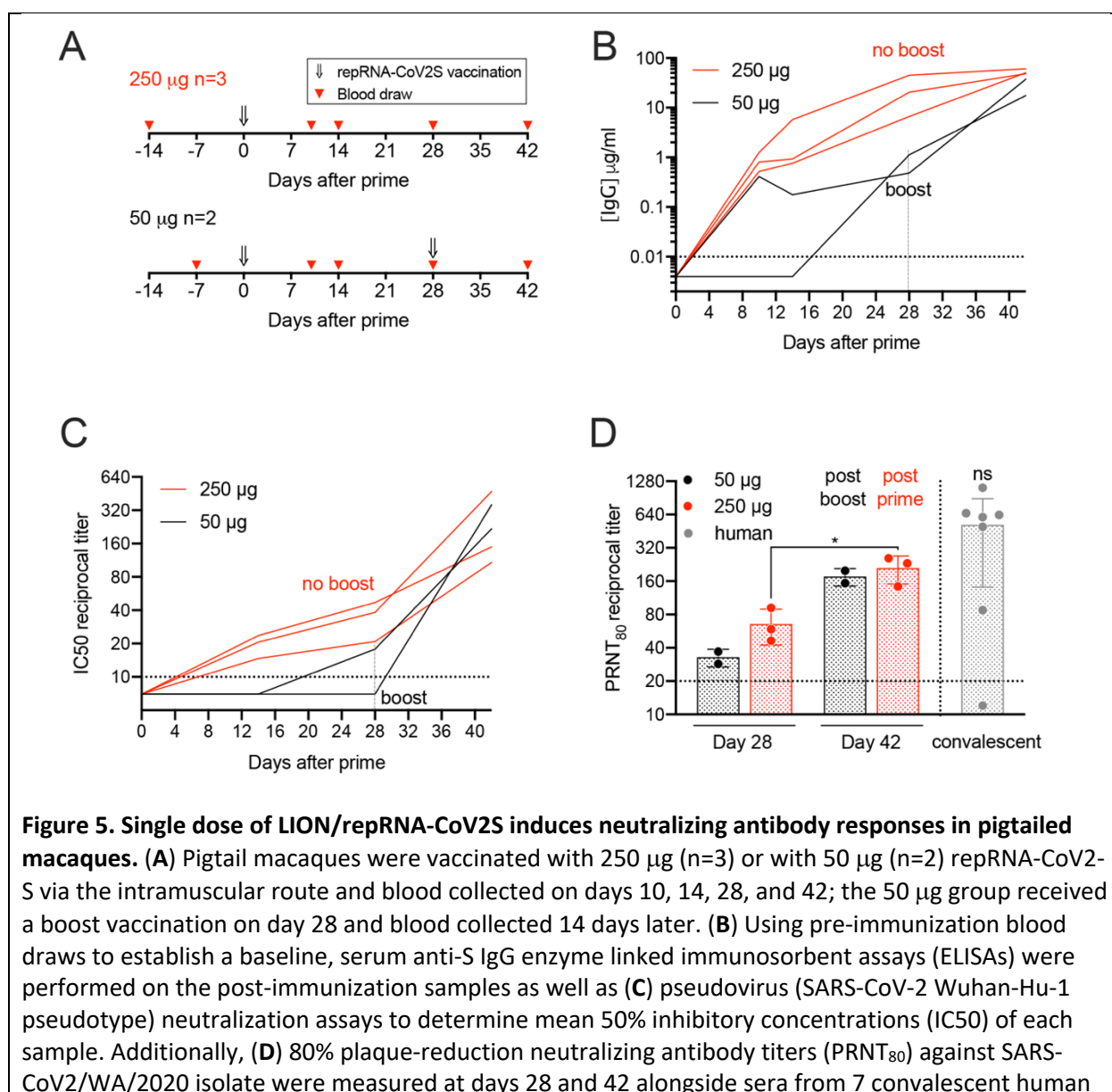


**Figure 4. LION/repRNA-CoV2S induces Th1-biased antibodies in aged BALB/C mice.** Two-, eight-, or seventeen-month old BALB/C mice (n=5/group) received 10 or 1  $\mu$ g LION/repRNA-CoV2S via the intramuscular route. Fourteen days after prime immunization, serum was harvested and (A) anti-S IgG or (B) IgG1 and IgG2a concentrations and (C) ratios were determined by enzyme-linked immunosorbent assay (ELISA). Data in 17-, 8-, and 2-month old BALB/Cs are from a single experiment and data for the 2-month old BALB/Cs were replicated in a second experiment. All data are represented as individual values as well as mean  $\pm$  s.d. \*p<0.05 as determined by one-way ANOVA with Tukey's multiple comparison test between the 17-month old animals and either the 8- or 2-month old animals.

121  
122 Having achieved robust immunogenicity with LION/repRNA-CoV2S in mice, we then immunized  
123 pigtail macaques (*Macaca nemestrina*) to determine if the vaccine was capable of inducing strong



124 immune responses in a nonhuman primate model that more closely resembles humans in the immune  
 125 response to vaccination. Three macaques received LION/repRNA-CoV2S at a single intramuscular 250  $\mu$ g  
 126 dose at week 0 and two macaques received a 50  $\mu$ g prime at week 0 and a boost at week 4. (Fig. 5A).  
 127 Blood was collected 10, 14, 28, and 42 days post vaccination to monitor vaccine safety and  
 128 immunogenicity. There were no observed reactions at the vaccine injection site nor adverse reactions in  
 129 the animals up to 42 days post-prime vaccination. Additionally, there were no abnormalities in weight or  
 130 temperature in the animals (Sup. Fig. 2A-B), and serum chemistries revealed no abnormal findings,  
 131 except for mild azotemia (mildly elevated blood urea nitrogen and creatinine) in 1 animal at 14 days  
 132 post vaccination (Sup. Fig. 2C). All CBC counts were unremarkable (Sup. Fig. 2D).



samples collected from confirmed COVID-19 patients (see Sup. Table 1). The experiment was performed once. Each line in **B** and **C** are representative of each individual animal. Data in **D** are reported as individual values as well as mean  $\pm$  s.d. \* $p < 0.05$  as determined by students t-test comparing 250  $\mu\text{g}$  groups at days 14 and 28. There was no significant difference (ns) between mean PRNT<sub>80</sub> titers in all 5 animals at day 42 and titers in sera from 7 convalescent humans, as measured by Mann-Whitney U test.

133  
134 ELISA analyses (Sup. Fig. 3) of sera collected 10, 14, 28, and 42 days after prime immunization  
135 showed that all three macaques immunized with the single 250  $\mu\text{g}$  dose seroconverted as early as day  
136 10, with anti-S IgG concentrations continuing to increase in these 3 animals to 48, 51, and 61  $\mu\text{g}/\text{ml}$  by  
137 day 42 (Fig. 5B). Both macaques receiving 50  $\mu\text{g}$  repRNA-CoV2S seroconverted after a single dose but  
138 developed significantly lower antibody responses with anti-S IgG concentrations of 1 and 0.5  $\mu\text{g}/\text{ml}$  by  
139 day 28, compared to 7, 20, and 45  $\mu\text{g}/\text{ml}$  in the 250  $\mu\text{g}$  group at this same time point (Fig. 5B).  
140 However, 14 days after a booster immunization, the 50  $\mu\text{g}$  group developed similar levels of anti-S IgG  
141 concentrations (18 and 37  $\mu\text{g}/\text{ml}$ ) as the 250  $\mu\text{g}$  prime-only group at this time point (48, 51, and 61  
142  $\mu\text{g}/\text{ml}$ ) (Fig. 5A). Additionally, sera from the three macaques immunized with just the single 250  $\mu\text{g}$   
143 dose neutralized pseudovirus (SARS-CoV-2 Wuhan-Hu-1 pseudotype) transduction of cells *in vitro* with  
144 reciprocal IC50 titers of 1:38, 1:20 and 1:47 by day 28 with levels increasing to 1:472, 1:108, and 1:149  
145 by day 42, whereas the 50  $\mu\text{g}$  group achieved similar robust IC50 titers only after the booster  
146 immunization reaching pseudovirus IC50 titers of 1:218 and 1:358 by day 42 (Fig. 5C and Sup. Fig. 4).  
147 Sera collected 28- and 42-days post vaccination were further analyzed for neutralization of wild type  
148 SARS-CoV-2/WA/2020 by 80% plaque reduction neutralization test (PRNT<sub>80</sub>) and compared to  
149 neutralizing titers in sera from convalescent humans collected 15-64 days following natural infection  
150 (Sup. Fig. 4 and Sup. Table 1). A single immunization with 50 and 250  $\mu\text{g}$  of LION/repRNA-CoV2S  
151 induced mean PRNT<sub>80</sub> titers of 1:32 and 1:66 by day 28, respectively. By Day 42, mean PRNT<sub>80</sub> titers  
152 significantly increased to 1:176 after a booster immunization in the 50  $\mu\text{g}$  group and to 1:211 in the  
153 prime-only 250  $\mu\text{g}$  group, (Fig. 5D and Sup. Fig. 4). Importantly, all 5 macaques developed PRNT<sub>80</sub> titers  
154 within the same range as titers measured in the seven convalescent humans (<1:20 to 1:1280, collected  
155 15 to 64 days post onset) and there was no significant difference in mean neutralizing titers between all  
156 5 vaccinated macaques (1:197) and convalescent humans (1:518) ( $P=0.27$ , Fig. 5D, Sup. Fig. 4, and Sup.  
157 Table 1). Recently, serum neutralizing titers, measured as the IC50 titer that neutralized SARS-CoV-2 by  
158 50% tissue culture infectious dose (TCID<sub>50</sub>), were reported in rhesus macaques that were either re-  
159 infected<sup>47</sup> or challenged after vaccination with an inactivated SARS-CoV-2 vaccine<sup>48</sup>. In the former  
160 report, IC50 titers as low as 1:8 were associated with protection from re-infection while in the latter,

161 IC50 titers as low as 1:50 were associated with reduced viral load and protection from lung pathology.  
162 These data suggest that a 250 µg prime-only or a 50 µg prime/boost immunization with the  
163 LION/repRNA-CoV2 vaccine may be able to induce levels of neutralizing antibodies sufficient to protect  
164 nonhuman primates from infection and disease. Studies are now underway to evaluate protective  
165 efficacy.

166 RepRNA vaccines against a variety of infectious diseases and cancers have been shown to be  
167 safe and potent in clinical trials<sup>49–52</sup>, and the cell-free and potentially highly scalable manufacturing  
168 process of repRNA when used with effective synthetic formulations, such as LION, present further  
169 benefits over mRNA. The two-vial approach provides a significant manufacturing and distribution  
170 advantage over LNP formulations that encapsulate RNA, as the vaccine can be stockpiled and combined  
171 onsite as needed. Additionally, we demonstrated that LION/repRNA-CoV-2 induces robust S-specific T  
172 cell responses in mice. Given the relatively recent emergence of SARS-CoV-2, we can only speculate  
173 based on limited knowledge from previous reports of coronavirus infection as to how T cell responses  
174 may contribute to protection from infection and disease. Following natural infection of humans with  
175 the related SARS-CoV, neutralizing antibody and memory B cell responses in some individuals are  
176 reported to be short lived (~ 3 years) while memory T cells persist at least 6 years<sup>53</sup>, suggesting a  
177 potential role for T cells in long term responses especially in those who lack robust memory B cell  
178 responses. Additionally, anti-S T-cell responses to the related SARS- and MERS-CoVs contribute towards  
179 viral clearance in normal as well as aged mice infected with SARS- or MERS-CoV, respectively<sup>43–45</sup>.

180 Together, our results demonstrate a significant potential for LION/repRNA-CoV2S, which will  
181 enter clinical development under the name HDT-301, to induce rapid immune protection from SARS-  
182 CoV-2 infection. A scalable and widely-distributed vaccine capable of inducing robust immunity in both  
183 young and aged populations against SARS-CoV-2 infection in a single shot would provide immediate  
184 and effective containment of the pandemic. Critically, the vaccine induced Th1-biased antibody and T  
185 cell responses in both young and aged mice, an attribute that has been associated with improved  
186 recovery and milder disease outcomes in SARS-CoV-infected patients<sup>54</sup>. Together, these results support  
187 further development of LION/repRNA-CoV2S as a vaccine candidate for protection from COVID19.

188

## 189 **Acknowledgements**

190 The authors would like to thank Briann Brown, Solomon Wangari, Joel Ahrens, Naoto Iwayama,  
191 and William Garrison for their technical assistance with the pigtail macaque study as well as Dr. Helen  
192 Chu and Sarah Bowell for donating remnant, de-identified convalescent human sera from confirmed

193 COVID-19 patients. Additionally, the authors thank Dr. Scott Weaver at the University of Texas Medical  
194 Branch for providing the plasmid vector encoding VEEV-TC83, and the Institute for Protein Design at the  
195 University of Washington for providing recombinant SARS-CoV-2 spike protein.

196 This work was funded by P51OD010425 (Washington National Primate Research Center),  
197 NIH/NIAID Centers of Excellence for Influenza Research and Surveillance contract HHSN27220140006C  
198 (JHE), and HDT Biotech internal funds. Additional support from the University of Washington Center for  
199 Innate Immunity and Immune Disease, NIH/NIAID contract 75N93019C00037 (MD), NIH/NIAID contract  
200 75N93019C00008 (APK), the NIGMS/NIH R01GM120553 (DV), NIAID/NIH HHSN272201700059C (DV), a  
201 Pew Biomedical Scholars Award (DV), an Investigators in the Pathogenesis of Infectious Disease Award  
202 from the Burroughs Wellcome Fund (DV), and the intramural research program of NIAID, NIH (DH, SL,  
203 HF). JHE is a Washington Research Foundation Postdoctoral fellow and is also supported by NIH  
204 1F32AI136371. The content is solely the responsibility of the authors and does not necessarily represent  
205 the official views of the funders.

#### 206 **Conflict of interest statement**

207 JHE, APK, JA, MD, DC, PB, MG, and SGR have equity interest in HDT Biocorp. JHE, PB, JF, DHF, HF and DH  
208 are inventors on a patent filing pertaining to repRNA-CoV2S. JHE, APK, DC, MD and SGR are inventors on  
209 a patent filing pertaining to LION formulation.

210 **References**

- 211 1. Lu, H., Stratton, C. W. & Tang, Y.-W. Outbreak of pneumonia of unknown etiology in Wuhan,  
212 China: The mystery and the miracle. *J. Med. Virol.* **92**, 401–402 (2020).
- 213 2. Wu, F. *et al.* A new coronavirus associated with human respiratory disease in China. *Nature* **579**,  
214 265–269 (2020).
- 215 3. Wang, C., Horby, P. W., Hayden, F. G. & Gao, G. F. A novel coronavirus outbreak of global health  
216 concern. *Lancet (London, England)* **395**, 470–473 (2020).
- 217 4. Hamming, I. *et al.* Tissue distribution of ACE2 protein, the functional receptor for SARS  
218 coronavirus. A first step in understanding SARS pathogenesis. *J. Pathol.* **203**, 631–637 (2004).
- 219 5. Letko, M., Marzi, A. & Munster, V. Functional assessment of cell entry and receptor usage for  
220 SARS-CoV-2 and other lineage B betacoronaviruses. *Nat. Microbiol.* **5**, 562–569 (2020).
- 221 6. Walls, A. C. *et al.* Structure, Function, and Antigenicity of the SARS-CoV-2 Spike Glycoprotein. *Cell*  
222 **181**, 281–292.e6 (2020).
- 223 7. Walls, A. C. *et al.* Unexpected Receptor Functional Mimicry Elucidates Activation of Coronavirus  
224 Fusion. *Cell* **176**, 1026–1039.e15 (2019).
- 225 8. Pinto, D. *et al.* Structural and functional analysis of a potent sarbecovirus neutralizing antibody.  
226 *bioRxiv* (2020) doi:10.1101/2020.04.07.023903.
- 227 9. He, Y., Lu, H., Siddiqui, P., Zhou, Y. & Jiang, S. Receptor-binding domain of severe acute  
228 respiratory syndrome coronavirus spike protein contains multiple conformation-dependent  
229 epitopes that induce highly potent neutralizing antibodies. *J. Immunol.* **174**, 4908–4915 (2005).
- 230 10. Jiang, S., He, Y. & Liu, S. SARS vaccine development. *Emerg. Infect. Dis.* **11**, 1016–1020 (2005).
- 231 11. Du, L. *et al.* The spike protein of SARS-CoV--a target for vaccine and therapeutic development.  
232 *Nat. Rev. Microbiol.* **7**, 226–236 (2009).
- 233 12. Menachery, V. D. *et al.* SARS-like WIV1-CoV poised for human emergence. *Proc. Natl. Acad. Sci.*  
234 *U. S. A.* **113**, 3048–3053 (2016).
- 235 13. Rockx, B. *et al.* Structural basis for potent cross-neutralizing human monoclonal antibody  
236 protection against lethal human and zoonotic severe acute respiratory syndrome coronavirus  
237 challenge. *J. Virol.* **82**, 3220–3235 (2008).
- 238 14. Traggiai, E. *et al.* An efficient method to make human monoclonal antibodies from memory B  
239 cells: potent neutralization of SARS coronavirus. *Nat. Med.* **10**, 871–875 (2004).
- 240 15. Corti, D. *et al.* Prophylactic and postexposure efficacy of a potent human monoclonal antibody  
241 against MERS coronavirus. *Proc. Natl. Acad. Sci. U. S. A.* **112**, 10473–10478 (2015).

- 242 16. Tseng, C.-T. *et al.* Immunization with SARS coronavirus vaccines leads to pulmonary  
243 immunopathology on challenge with the SARS virus. *PLoS One* **7**, e35421 (2012).
- 244 17. Honda-Okubo, Y. *et al.* Severe Acute Respiratory Syndrome-Associated Coronavirus Vaccines  
245 Formulated with Delta Inulin Adjuvants Provide Enhanced Protection while Ameliorating Lung  
246 Eosinophilic Immunopathology. *J. Virol.* **89**, 2995–3007 (2015).
- 247 18. Thanh Le, T. *et al.* The COVID-19 vaccine development landscape. *Nature reviews. Drug discovery*  
248 (2020) doi:10.1038/d41573-020-00073-5.
- 249 19. Shang, W., Yang, Y., Rao, Y. & Rao, X. The outbreak of SARS-CoV-2 pneumonia calls for viral  
250 vaccines. *npj Vaccines* **5**, 18 (2020).
- 251 20. Xiong, C. *et al.* Sindbis virus: an efficient, broad host range vector for gene expression in animal  
252 cells. *Science (80-. )*. **243**, 1188 LP – 1191 (1989).
- 253 21. Zhou, X. *et al.* Self-replicating Semliki Forest virus RNA as recombinant vaccine. *Vaccine* **12**, 1510–  
254 1514 (1994).
- 255 22. Ljungberg, K. & Liljeström, P. Self-replicating alphavirus RNA vaccines. *Expert Rev. Vaccines* **18**, 1-  
256 18 [Epub ahead of print] (2014).
- 257 23. Frolov, I. *et al.* Alphavirus-based expression vectors: strategies and applications. *Proc. Natl. Acad.*  
258 *Sci.* **93**, 11371–11377 (2002).
- 259 24. Bredenbeek, P. J., Frolov, I., Rice, C. M. & Schlesinger, S. Sindbis virus expression vectors:  
260 packaging of RNA replicons by using defective helper RNAs. *J. Virol.* **67**, 6439–6446 (1993).
- 261 25. Liljestrom, P. & Garoff, H. A new generation of animal cell expression vectors based on the  
262 Semliki Forest virus replicon. *Biotechnology. (N. Y.)*. **9**, 1356–1361 (1991).
- 263 26. Pushko, P. *et al.* Replicon-helper systems from attenuated Venezuelan equine encephalitis virus:  
264 expression of heterologous genes in vitro and immunization against heterologous pathogens in  
265 vivo. *Virology* **239**, 389–401 (1997).
- 266 27. Berglund, P., Smerdou, C., Fleeton, M. N., Tubulekas, I. & Liljestrom, P. Enhancing immune  
267 responses using suicidal DNA vaccines. *Nat. Biotechnol.* **16**, 562–565 (1998).
- 268 28. Jensen, S. & Thomsen, a. R. Sensing of RNA Viruses: a Review of Innate Immune Receptors  
269 Involved in Recognizing RNA Virus Invasion. *J. Virol.* **86**, 2900–2910 (2012).
- 270 29. Vogel, A. B. *et al.* Self-Amplifying RNA Vaccines Give Equivalent Protection against Influenza to  
271 mRNA Vaccines but at Much Lower Doses. *Mol. Ther.* **26**, 446–455 (2018).
- 272 30. Strauss, J. H. & Strauss, E. G. The alphaviruses: gene expression, replication, and evolution.  
273 *Microbiol. Rev.* **58**, 491–562 (1994).



- 274 31. Kinney, R. M. *et al.* Attenuation of Venezuelan equine encephalitis virus strain TC-83 is encoded  
275 by the 5'-noncoding region and the E2 envelope glycoprotein. *J. Virol.* **67**, 1269–1277 (1993).
- 276 32. Atasheva, S. *et al.* Pseudoinfectious Venezuelan Equine Encephalitis Virus: a New Means of  
277 Alphavirus Attenuation. *J. Virol.* **87**, 13 (2016).
- 278 33. Erasmus, J. H. *et al.* A Nanostructured Lipid Carrier for Delivery of a Replicating Viral RNA  
279 Provides Single, Low-Dose Protection against Zika. *Mol. Ther.* **26**, 1–16 (2018).
- 280 34. Duthie, M. S. *et al.* Heterologous Immunization With Defined RNA and Subunit Vaccines  
281 Enhances T Cell Responses That Protect Against *Leishmania donovani*. *Front. Immunol.* **9**, 2420  
282 (2018).
- 283 35. Calabro, S. *et al.* The adjuvant effect of MF59 is due to the oil-in-water emulsion formulation,  
284 none of the individual components induce a comparable adjuvant effect. *Vaccine* **31**, 3363–3369  
285 (2013).
- 286 36. Desbien, A. L. *et al.* Squalene emulsion potentiates the adjuvant activity of the TLR4 agonist, GLA,  
287 via inflammatory caspases, IL-18, and IFN- $\gamma$ . *Eur. J. Immunol.* **45**, 407–417 (2015).
- 288 37. Yu, E. Y. *et al.* Magnetic Particle Imaging for Highly Sensitive, Quantitative, and Safe in Vivo Gut  
289 Bleed Detection in a Murine Model. *ACS Nano* **11**, 12067–12076 (2017).
- 290 38. Khandhar, A. P. *et al.* Evaluation of PEG-coated iron oxide nanoparticles as blood pool tracers for  
291 preclinical magnetic particle imaging. *Nanoscale* **9**, 1299–1306 (2017).
- 292 39. Bauer, L. M., Situ, S. F., Griswold, M. A. & Samia, A. C. S. High-performance iron oxide  
293 nanoparticles for magnetic particle imaging - guided hyperthermia (hMPI). *Nanoscale* **8**, 12162–  
294 12169 (2016).
- 295 40. Zhao, Y., Zhao, X., Cheng, Y., Guo, X. & Yuan, W. Iron Oxide Nanoparticles-Based Vaccine Delivery  
296 for Cancer Treatment. *Mol. Pharm.* **15**, 1791–1799 (2018).
- 297 41. Zanganeh, S. *et al.* Iron oxide nanoparticles inhibit tumour growth by inducing pro-inflammatory  
298 macrophage polarization in tumour tissues. *Nat. Nanotechnol.* **11**, 986–994 (2016).
- 299 42. Khandhar, A. P. *et al.* Evaluating size-dependent relaxivity of PEGylated-USPIOs to develop  
300 gadolinium-free T1 contrast agents for vascular imaging. *J. Biomed. Mater. Res. A* **106**, 2440–  
301 2447 (2018).
- 302 43. Zhao, J., Zhao, J. & Perlman, S. T cell responses are required for protection from clinical disease  
303 and for virus clearance in severe acute respiratory syndrome coronavirus-infected mice. *J. Virol.*  
304 **84**, 9318–9325 (2010).
- 305 44. Channappanavar, R., Zhao, J. & Perlman, S. T cell-mediated immune response to respiratory

- 306 coronaviruses. *Immunol. Res.* **59**, 118–128 (2014).
- 307 45. Channappanavar, R., Fett, C., Zhao, J., Meyerholz, D. K. & Perlman, S. Virus-Specific Memory CD8  
308 T Cells Provide Substantial Protection from Lethal Severe Acute Respiratory Syndrome  
309 Coronavirus Infection. *J. Virol.* **88**, 11034–11044 (2014).
- 310 46. Mills, C. D., Kincaid, K., Alt, J. M., Heilman, M. J. & Hill, A. M. M-1/M-2 Macrophages and the  
311 Th1/Th2 Paradigm. *J. Immunol.* **164**, 6166–6173 (2000).
- 312 47. Bao, L. *et al.* Reinfection could not occur in SARS-CoV-2 infected rhesus macaques. *bioRxiv*  
313 2020.03.13.990226 (2020) doi:10.1101/2020.03.13.990226.
- 314 48. Gao, Q. *et al.* Development of an inactivated vaccine candidate for SARS-CoV-2. *Science (80-. )*.  
315 **1932**, eabc1932 (2020).
- 316 49. Bernstein, D. I. *et al.* Randomized, double-blind, Phase 1 trial of an alphavirus replicon vaccine for  
317 cytomegalovirus in CMV seronegative adult volunteers. *Vaccine* **28**, 484–493 (2009).
- 318 50. Hubby, B. *et al.* Development and preclinical evaluation of an alphavirus replicon vaccine for  
319 influenza. *Vaccine* **25**, 8180–8189 (2007).
- 320 51. Morse, M. A. *et al.* Phase I study of alphaviral vector (AVX701) in colorectal cancer patients:  
321 comparison of immune responses in stage III and stage IV patients. *J. Immunother. Cancer* **3**,  
322 P444–P444 (2015).
- 323 52. Reap, E. A. *et al.* Development and preclinical evaluation of an alphavirus replicon particle  
324 vaccine for cytomegalovirus. *Vaccine* **25**, 7441–7449 (2007).
- 325 53. Tang, F. *et al.* Lack of Peripheral Memory B Cell Responses in Recovered Patients with Severe  
326 Acute Respiratory Syndrome: A Six-Year Follow-Up Study. *J. Immunol.* **186**, 7264–7268 (2011).
- 327 54. Li, C. K. *et al.* T Cell Responses to Whole SARS Coronavirus in Humans. *J. Immunol.* **181**, 5490–  
328 5500 (2008).
- 329
- 330

## 331 **Supplementary Material**

### 332 **Materials and Methods**

333 ***SARS-CoV-2 repRNA vaccine production and qualification.*** Codon optimized gene sequences  
334 for SARS-CoV-2 full S corresponding to positions 21,536 to 25,384 in SARS-CoV-2 isolate Wuhan-  
335 Hu-1 (GenBank: MN908947.3) fused to a c-terminal v5 epitope tag was synthesized as double  
336 stranded DNA fragments (IDT) and cloned into a plasmid vector encoding the 5' and 3'  
337 untranslated regions as well as the nonstructural open reading frame of Venezuelan equine  
338 encephalitis virus, strain TC-83, between PflFI and SacII sites by Gibson assembly (SGI-DNA).  
339 Clones were then sanger sequenced and prepped for RNA production as follows. Template DNA  
340 was linearized by enzymatic digestion with NotI followed by phenol chloroform treatment and  
341 ethanol precipitation. Linearized template was transcribed using MEGAscript® T7 Transcription  
342 Kit (Invitrogen, Carlsbad, CA) followed by capping with NEB Vaccinia Capping System as  
343 previously described<sup>1</sup>. To qualify the vaccine candidate *in vitro*, Baby Hamster Kidney (BHK)  
344 cells (ATCC) were transfected with repRNA or mock transfected using *TransIT-mRNA*  
345 transfection kit (Mirus Bio) and cells analyzed 24 hours later by immunofluorescence using a  
346 mouse anti-v5 AF488 secondary antibody (Invitrogen). Additionally, BHK cells were transfected  
347 with repRNA-CoV2S and repRNA-GFP and cell lysates were collected 24 hours later for analysis  
348 by SDS-PAGE and by western blot using recombinant SARS-CoV-2 S protein as a positive control.  
349 To detect repRNA-mediated protein expression following transfer to nitrocellulose membrane,  
350 anti-v5-HRP or convalescent human serum collected 29 days after onset of PCR-confirmed  
351 COVID-19 followed by anti-human Ig-HRP secondary antibody (Southern Biotech) was used.

352 ***LION formulation.*** To protect the RNA replicons from degradation, we partnered them with a  
353 Lipid InOrganic Nanoparticle (LION) formulation that consists of inorganic superparamagnetic  
354 iron oxide (SPIO) nanoparticles within a hydrophobic squalene core to enhance formulation  
355 stability. LIONS comprise 37.5 mg/ml squalene (Millipore Sigma), 37 mg/ml Span® 60 (Millipore  
356 Sigma), 37 mg/ml Tween® 80 (Fisher Chemical), 30 mg/ml DOTAP chloride (Corden Pharma), 0.2  
357 mg/ml 15 nm oleic acid-coated iron oxide nanoparticles (Ocean Nanotech, San Diego, CA) and  
358 10 mM sodium citrate dihydrate (Fisher Chemical). LION particles were manufactured by

359 combining the iron oxide nanoparticles with the oil phase (Squalene, Span 60, and DOTAP) and  
360 sonicating for 30 minutes in a 65°C water bath. Separately, the aqueous phase, containing  
361 Tween 80 and sodium citrate dihydrate solution in water, was prepared with continuous stirring  
362 until all components were dissolved. The oil and aqueous phases were then mixed and  
363 emulsified using a VWR 200 homogenizer (VWR International) and the crude colloid was  
364 subsequently processed by passaging through a microfluidizer at 20,000 psi with a LM10  
365 microfluidizer equipped with a H10Z-100 µm ceramic interaction chamber (Microfluidics) until  
366 the z-average hydrodynamic diameter – measured by dynamic light scattering (Malvern  
367 Zetasizer Nano S) – reached 50 ±5 nm with a 0.2 polydispersity index. The microfluidized LION  
368 was terminally filtered with a 200 nm pore-size polyethersulfone (PES) filter and stored at 2-  
369 8°C.

370 ***RNase protection.*** Replicon RNA was complexed with LION formulations and placed on ice for  
371 30 min. After diluting the complex using nuclease-free water, complexes containing 1 µg of  
372 repRNA at 20 µg/mL were treated with 50 ng of RNase A (Thermo Scientific) for 30 min at room  
373 temperature, followed by an incubation with 5 µg of recombinant Proteinase K (Thermo  
374 Scientific) for 10 min at 55°C. RNA was then extracted using an equal volume of 25:24:1  
375 phenol:chloroform:isoamyl alcohol (Invitrogen). After vortexing, samples were centrifuged at  
376 17,000 × *g* for 15 min. The supernatant was collected and mixed 1:1 with Glyoxal load dye  
377 (Invitrogen) and heated at 50°C for 15 min. The equivalent of 200 ng of RNA was loaded and run  
378 on a denatured 150 mL 1% agarose gel in Northern Max Gly running buffer (Invitrogen) at 120 V  
379 for 45 min. Gels were imaged using a ChemiDoc MP imaging system (BioRad). The intensity of  
380 the intact RNA band was compared to phenol:chloroform:isoamyl extracted RNA from  
381 complexes that were not subjected to RNase and Proteinase K treatment.

382  
383 ***Mouse immunizations.*** All mouse experiments were conducted in accordance with procedures  
384 approved by the institutional animal care and use committee. Female C57BL/6 or BALB/C mice  
385 (purchased from Charles River, Wilmington, MA) were maintained in specific pathogen-free  
386 conditions and entered experiments at 6-12 weeks of age unless otherwise indicated. Mice  
387 were immunized by intramuscular injection of vaccine delivered in a total volume of 50 µl in the

388 thigh.

389

390 ***Pigtail macaque study.*** Five adult male pigtail macaques were used in these studies (aged 3-6  
391 years, weight 5-13 kg). All animals received a previous Hepatitis B virus (HBV) DNA and protein  
392 vaccine regimen, comprised of HBV core and surface antigens and anti-CD180<sup>2</sup>, and were re-  
393 enrolled in this study in response to the SARS-CoV-2 pandemic. All animals were housed at the  
394 Washington National Primate Research Center (WaNPRC), an accredited by the American  
395 Association for the Accreditation of Laboratory Animal Care International (AAALAC), and as  
396 previously described<sup>3</sup>. All procedures performed on the animals were with the approval of the  
397 University of Washington's Institutional Animal Care and Use Committee (IACUC).

398 Blood was collected at baseline (week -2 or -1), and at days 10, 14, 28, and 42 post-  
399 prime vaccination (Fig. 5A). Blood was also collected 10 days post-boost (38 days post-prime) in  
400 the 50µg vaccinated animals. Serum and plasma were collected and PBMCs were isolated from  
401 whole blood as previously described<sup>4</sup>. Animals were sedated with an intramuscular injection  
402 (10 mg/kg) of ketamine (Ketaset®; Henry Schein) prior to blood collection or vaccination.  
403 Animals were observed daily for general health (activity, appetite) and for evidence of  
404 reactogenicity at the vaccine inoculation site (swelling, redness). They also received full physical  
405 exams including temperature and weights measurements at each study timepoint. None of the  
406 animals became severely ill during the course of the study and none required euthanasia.

407

408 ***Pigtail macaque immunization.*** LION and repRNA-CoV2S were complexed at a nitrogen-to-  
409 phosphate molar ratio of 15 in 10mM sodium citrate and 20% sucrose buffer on ice and  
410 incubated for at least 30 minutes. The 50µg vaccine was delivered intramuscularly into the  
411 quadriceps muscle with one 250 µl injection on weeks 0 and 4. The 250µg vaccine was  
412 delivered intramuscularly with five 250µl injections over 4 muscles, 2 in the right quadriceps, 1  
413 in the left quadricep, and 1 each in the left and right deltoids on week 0. All injection sites were  
414 shaved prior to injection and monitored post-injection for any signs of local reactogenicity.

415

416 ***Serum Chemistries and Complete Blood Counts.*** Serum chemistries were run on a Beckman

417 Coulter AU 680/5812 system and complete blood counts were determined on a Sysmex XN9000  
418 analyzer by the University of Washington Department of Laboratory Medicine.

419  
420 **Antigen-specific antibody responses.** Blood was collected from the retro-orbital sinus of  
421 immunized mice, or venipuncture of anesthetized macaques, and serum prepared. Antigen-  
422 specific IgG, IgG1, IgG2a, and IgG2c responses were detected by enzyme linked immunosorbent  
423 assay (ELISA) using a previously described recombinant SARS-CoV-2 S as the capture antigen <sup>5</sup>.  
424 ELISA plates (Nunc, Rochester, NY) were coated with 1 µg/ml antigen or with serial dilutions of  
425 purified polyclonal IgG from mouse or monkeys to generate a standard curve in 0.1 M PBS  
426 buffer and blocked with 0.2% BSA-PBS. Then, in consecutive order, washes in PBS/Tween,  
427 serially diluted serum samples, anti-mouse or-monkey IgG, IgG1, IgG2a, or IgG2c-HRP (Southern  
428 Biotech, Birmingham, AL) and TMB then HCL were added to the plates. Plates were analyzed at  
429 405nm (ELx808, Bio-Tek Instruments Inc, Winooski, VT). Absorbance values from the linear  
430 segment of each serum dilution curve was used to interpolate the standard curve and calculate  
431 the IgG concentration present in each sample.

432  
433 **SARS-CoV-2 pseudovirus neutralization.** Murine leukemia virus (MLV)-based SARS-CoV-2 S-  
434 pseudotyped viruses were prepared as previously described <sup>5,6</sup>. In brief, HEK293T cells were co-  
435 transfected with a SARS-CoV-2 (based on Wuhan-Hu-1 isolate) S-encoding plasmid, an MLV  
436 Gag-Pol packaging construct, and the MLV transfer vector encoding a luciferase reporter using  
437 the Lipofectamine 2000 transfection reagent (Life Technologies) according to the  
438 manufacturer's instructions. Cells were incubated for 5 hours at 37°C with 8% CO<sub>2</sub> with DNA,  
439 lipofectamine, and OPTIMEM transfection medium. Following incubation DMEM containing  
440 10% FBS was added for 72 hours. Pseudovirus was then concentrated using a 30kDa Amicon  
441 concentrator for 10 minutes at 3,000 x g and frozen at -80C.

442 BHK cells were plated in 96 well plates for 16-24 hours prior to being transfected with  
443 human ACE2 using standard lipofectamine 2000 protocol and incubated for 5 hours at 37°C  
444 with 8% CO<sub>2</sub> with DNA, lipofectamine, and OPTIMEM transfection medium. Following  
445 incubation, DMEM containing 20% FBS was added in equal volume to the OPTIMEM



446 transfection media for 16-24 hours. Concentrated pseudovirus with or without serial dilution of  
447 antibodies was incubated for 1 hour at room temperature and then added to the wells after  
448 washing 3X with DMEM and removing all media. After 2-3 hours, equal volumes of DMEM  
449 containing 20% FBS and 2% PenStrep was added to the cells for 48 hours. Following 48 hours of  
450 infection, equal volume of One-Glo-EX (Promega) was added to the cells and incubated in the  
451 dark for 5-10 minutes prior to reading on a Varioskan LUX plate reader (ThermoFisher).  
452 Measurements were done in duplicate and relative luciferase units (RLU) were recorded.

453  
454 **SARS-CoV-2 neutralization.** Three-fold (pigtail macaque) or four-fold (human) serial dilutions of  
455 heat inactivated serum and 600 plaque-forming units (PFU)/ml solution of SARS-CoV-2/WA/20  
456 (BEI resources) were mixed 1:1 in DPBS (Fisher Scientific) + 0.3% gelatin (Sigma G7041) and  
457 incubated for 30 min at 37°C. Serum/virus mixtures were added in duplicate, along with virus  
458 only and mock controls, to Vero E6 cells (ATCC) in a 12-well plate and incubated for 1hr at 37°C.  
459 Following adsorption, plates were washed once with DPBS and overlaid with a 1:1 mixture of  
460 Avicel RC-591 (FMC) + 2 x MEM (ThermoFisher) supplemented with 4% heat-inactivated FBS  
461 and Penicillin/Streptomycin (Fisher Scientific). Plates were then incubated for 2 days at 37°C.  
462 Following incubation, overlay was removed and plates were washed once with DPBS and then  
463 10% formaldehyde (Sigma-Aldrich) in DPBS was added to cells and incubated for 30 minutes at  
464 room temp. Plates were washed again with DPBS and stained with 1% crystal violet (Sigma-  
465 Aldrich) in 20% EtOH (Fisher Scientific). Plaques were enumerated and percent neutralization  
466 was calculated relative to the virus-only control.

467  
468 **Mouse IFN- $\gamma$  ELISPOT.** Spleen and lung lymphocytes were isolated from mice 12 days after the  
469 second vaccination. MIAPS4510-Multiscreen plates (Millipore) were coated with rat anti mouse  
470 IFN-gamma capture antibody (BD) in PBS and incubated overnight at 4°C. The plates were  
471 washed in PBS and then blocked (2h, RT) with RPMI medium (Invitrogen) containing 10% heat  
472 inactivated fetal calf serum (Gibco). Lung and spleen cells were plated at  $5 \times 10^5$  and  $2.5 \times 10^5$   
473 cells/well and stimulated with the SARS-Cov2 S peptide pools (11aa overlapping 15 mer  
474 peptides from Genscript) at 1.5  $\mu\text{g/ml}$ /peptide and cultured for 20 hours (37°C, 5% CO<sub>2</sub>).

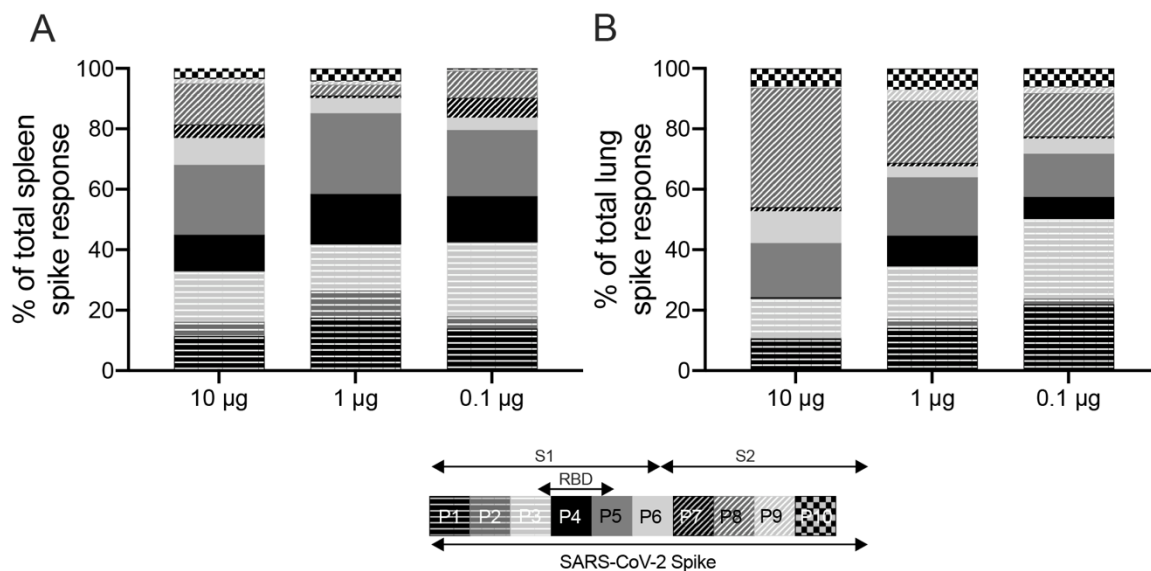
475 Biotinylated anti-mouse IFN-gamma antibody (BD) and streptavidin-Alkaline Phosphatase-  
476 substrate (Biolegend) were used to detect IFN-gamma secreting cells. Spot forming cells were  
477 enumerated using an Immunospot Analyzer from CTL Immunospot profession software  
478 (Cellular Technology Ltd).

479

480 **Statistical analyses.** Statistical analyses were conducted in Prism (Graphpad) using one-way  
481 analysis of variance and Tukey's multiple comparison test used to compare more than two  
482 groups, and either student's t or Mann Whitney U tests to compare two groups. Statistical  
483 significance was considered when the  $p$ -values were  $< 0.05$ .

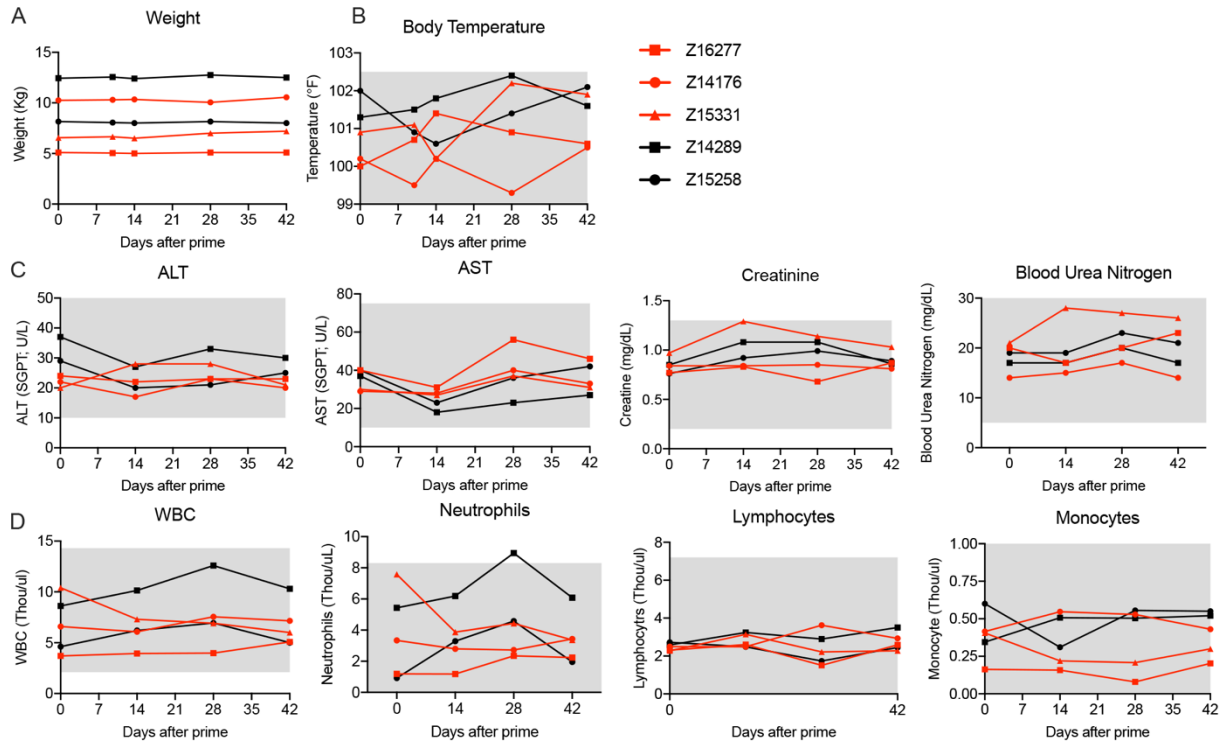
484 **Data availability.** Data have been deposited in Figshare: [10.6084/m9.figshare.12385574](https://figshare.com/10.6084/m9.figshare.12385574)

485 **Supplemental Figures**



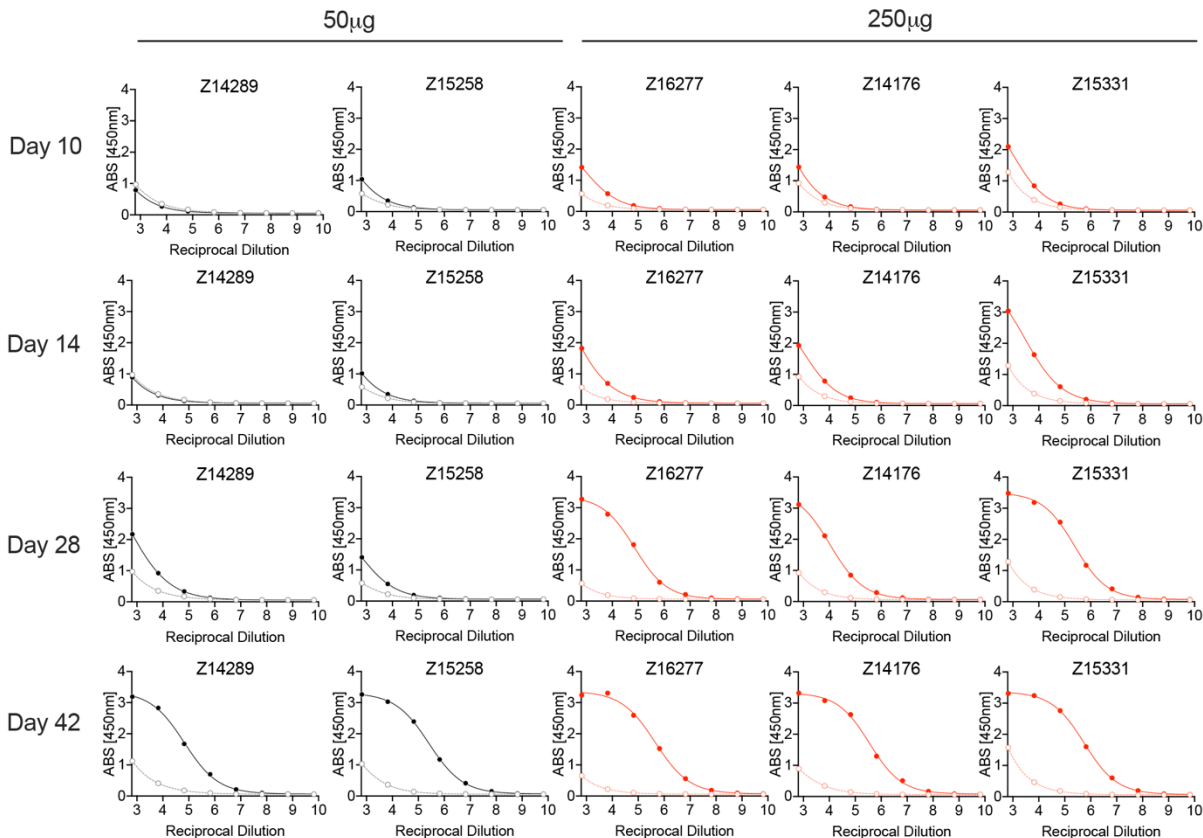
**Supplemental Figure 1. Breadth of T-cell responses in C57BL/6 mice.** Six to eight-week old C57BL/6 mice (n=5/group) received 10, 1, or 0.1 µg LION/repRNA-CoV2S via the intramuscular route. On day 28, mice received a booster immunization and 12 days later, **(A)** spleens and **(B)** lungs were harvested and IFN- $\gamma$  responses were measured by enzyme-linked immune absorbent spot (ELISpot) following stimulation with 10 peptide pools encompassing the entire Spike protein. Each peptide pool consisted of 26-29 15-mer peptides overlapping by 11 amino acids. Data are presented as percent of total spike response.

486

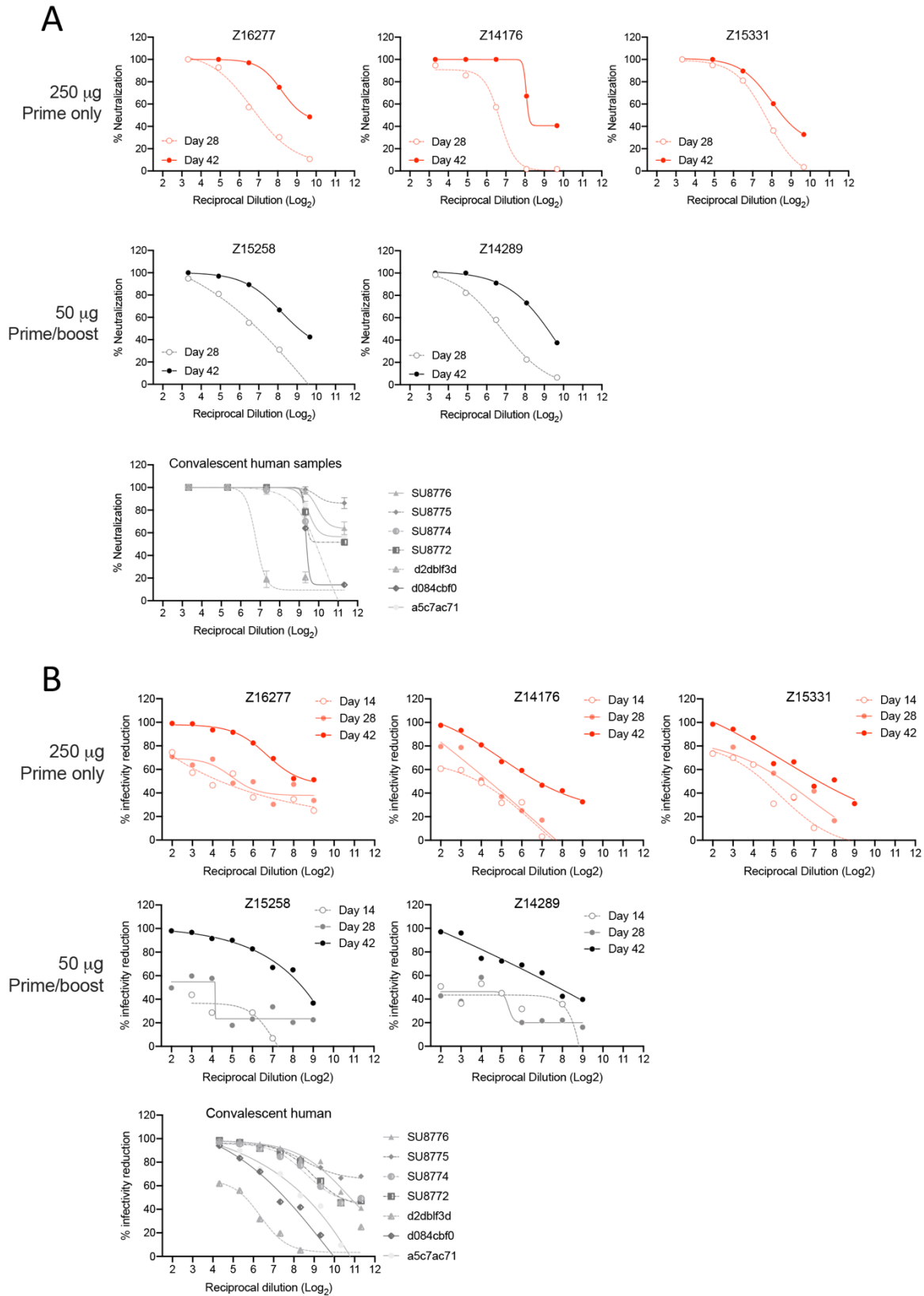


**Supplemental Figure 2. Vaccination did not induce adverse reactions in pigtail macaques. (A).** Body weight in kg. **(B)** Rectal body temperature in Fahrenheit. **(C)** Serum chemistries. **(D)** Blood complete blood counts (CBC). **(A-D)** Grey shaded areas indicate normal ranges for pigtail macaques.

487



**Supplemental Figure 3. Raw ELISA absorbance values from pigtail macaque study.** Recombinant SARS-CoV-2, based on the Wuhan-Hu-1 isolate, was used as the capture antigen and goat anti-monkey IgG-HRP used as the secondary conjugate. Absorbance values were determined at 405nm. Data are presented as pre-immune sera (open circles, dotted line) with post-immune sera (closed circles, solid line). Data are presented as pre-immune sera (open circles, dotted line) with post-immune sera (closed circles, solid line).





**Supplemental Figure 4. Neutralization curves of pigtail macaque and human samples against (A)**

**SARS-CoV-2/WA/2020 or (B) pseudotyped virus.** SARS-CoV-2/WA/2020 neutralization was

performed on sera collected from macaques on days 28 and 42 post-primary immunization.

Pseudoviral (SARS-CoV-2 Wuhan-Hu-1 pseudotype) neutralization was performed on sera collected from macaques on days 14, 28, and 42 post-primary. (see Sup. Table 1). Both assays were performed alongside sera from 7 convalescent humans collected at various timepoints after their first positive test for SARS-CoV-2 infection.

489

**Supplemental Table 1. Convalescent sera from COVID-19 patients**

<b>Sample ID</b>	<b>Days post onset</b>	<b>PRNT<sub>80</sub></b>
SU8776	20	1119
SU8775	15	<20
SU8774	21	496
SU8772	unknown	635
d2db1f3d	35	88
d084cbf0	29	607
a5c7ac71	64	658

490

491 **Supplemental References**

- 492 1. Erasmus, J. H. *et al.* A Nanostructured Lipid Carrier for Delivery of a Replicating Viral RNA  
493 Provides Single, Low-Dose Protection against Zika. *Mol. Ther.* **26**, 2507–2522 (2018).
- 494 2. Chaplin, J. W., Chappell, C. P. & Clark, E. A. Targeting antigens to CD180 rapidly induces  
495 antigen-specific IgG, affinity maturation, and immunological memory. *J. Exp. Med.* **210**,  
496 2135–2146 (2013).
- 497 3. Munson, P. *et al.* Therapeutic conserved elements (CE) DNA vaccine induces strong T-cell  
498 responses against highly conserved viral sequences during simian-human  
499 immunodeficiency virus infection. *Hum. Vaccin. Immunother.* **14**, 1820–1831 (2018).
- 500 4. O'Connor, M. A. *et al.* Mucosal T Helper 17 and T Regulatory Cell Homeostasis Correlate  
501 with Acute Simian Immunodeficiency Virus Viremia and Responsiveness to Antiretroviral  
502 Therapy in Macaques. *AIDS Res. Hum. Retroviruses* **35**, 295–305 (2019).
- 503 5. Walls, A. C. *et al.* Structure, function and antigenicity of the SARS-CoV-2 spike  
504 glycoprotein. *bioRxiv* 2020.02.19.956581 (2020) doi:10.1101/2020.02.19.956581.
- 505 6. Millet, J. K. & Whittaker, G. R. Murine Leukemia Virus (MLV)-based Coronavirus Spike-  
506 pseudotyped Particle Production and Infection. *Bio-protocol* **6**, e2035 (2016).

507

508